

# Study of Periodicity in Blazar Light Curves with a Machine Learning Approach

Paolo Cristarella Orestano<sup>1 2</sup>

Prof. Gino Tosti<sup>1 2</sup>, Dr. Sara Cutini<sup>2</sup>, Dr. Stefano Germani<sup>1 2</sup>

<sup>1</sup> University of Perugia

<sup>2</sup> INFN Perugia



# Outline

---

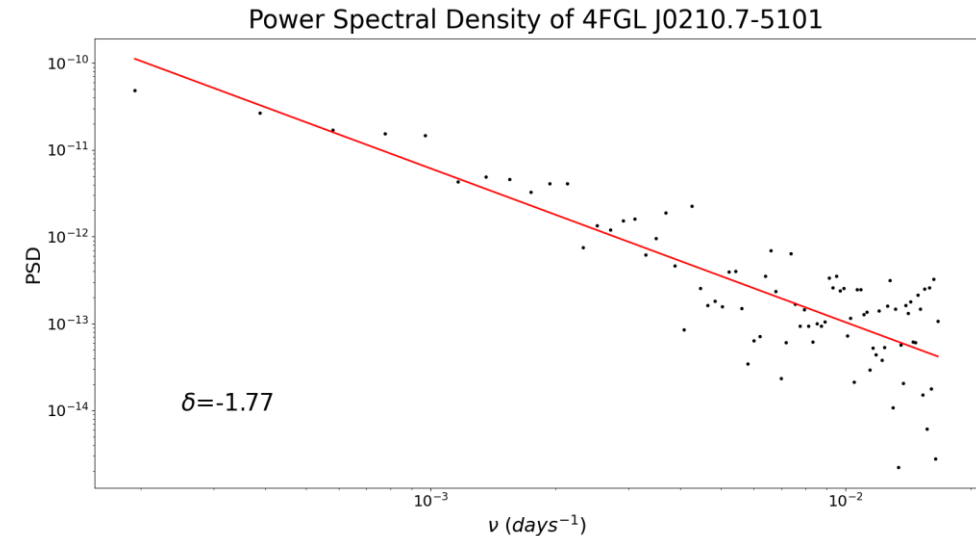
- **Blazar Variability and Periodicity**
- **Sources**
- **Analysis**
  - Weighted Wavelet Z-transform
  - Lomb Scargle Periodogram
  - Time Series and Noise Simulations
  - Emmanoulopoulos Simulations
- **Machine Learning**
- **Outlook**

# Blazar Variability and Periodicity

Large variability at various wavelengths.

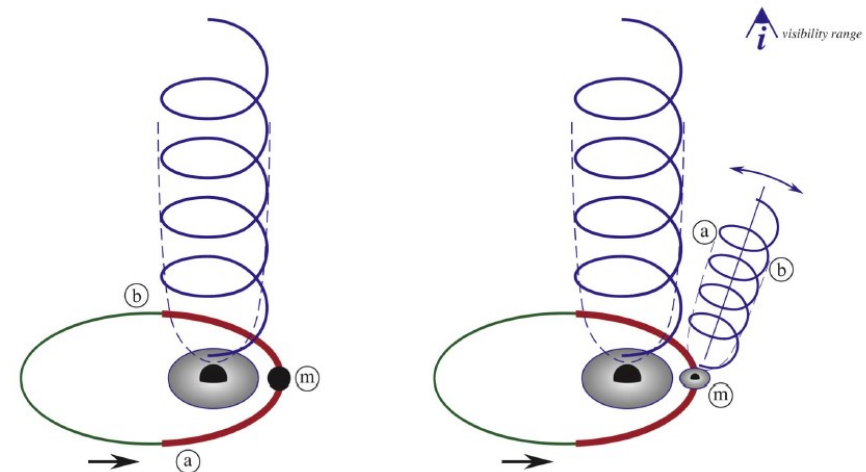
**Pink** or **red noise** type power spectrum  $\propto f^\delta$ .

The parameter  $\delta$  goes from  $\delta = -0.5$  to  $\delta = -2$ .



Long-term periodicities, or Quasi Periodic Oscillation, QPO, (founded in previous works [1][2]) could be related to **binary black holes** [3]:

- Intensity modulation.
- Precession, deflection or curvature of the jet changing the viewing angle.
- Not one but two jets.



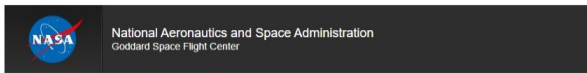
Tavani et al., 2018 [4]



# Sources

From the [Light Curve Repository](https://fermi.gsfc.nasa.gov/ssc/data/access/lat/LightCurveRepository/)<sup>1</sup> **1525**  $\gamma$ -ray **sources** analyzed: 571 FSRQ, 476 BLL, 371 unknown types of blazars, 107 other sources.

**Six** light curves **data types**: Energy flux (free index), Photon Flux (fixed index), 30d, 7d and 3d sampling.

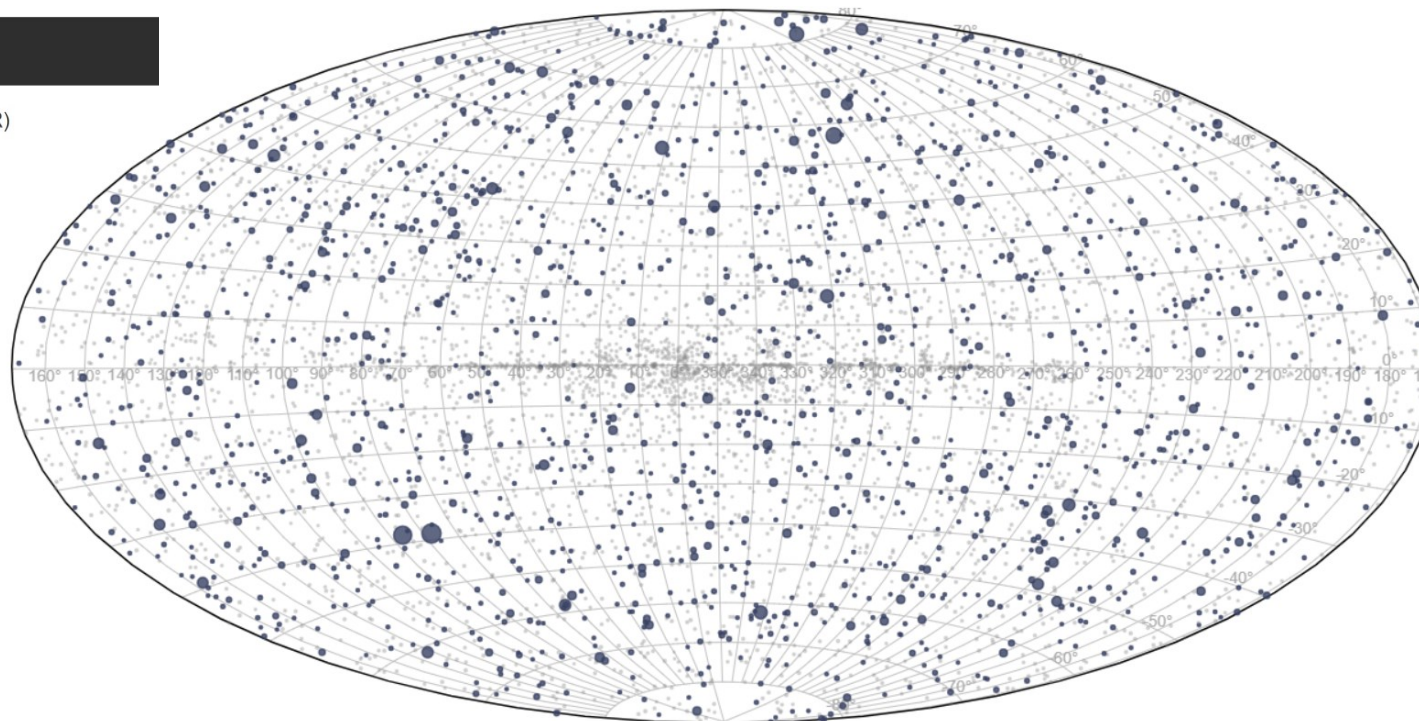


Fermi LAT Light Curve Repository (LCR)

Catalog Search

RA:  Dec:  Radius:

Keyword:

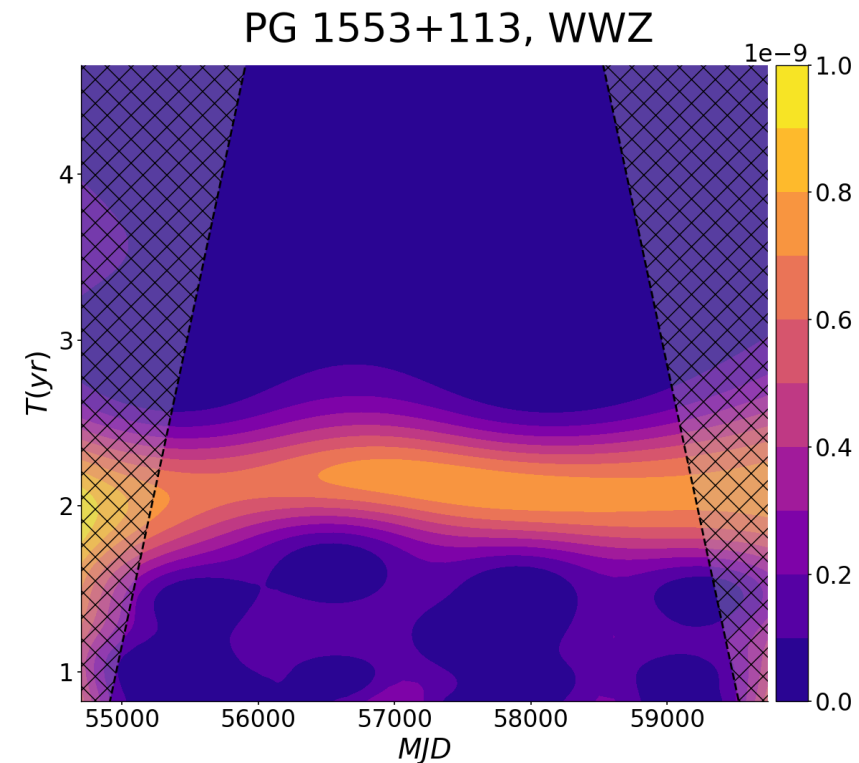
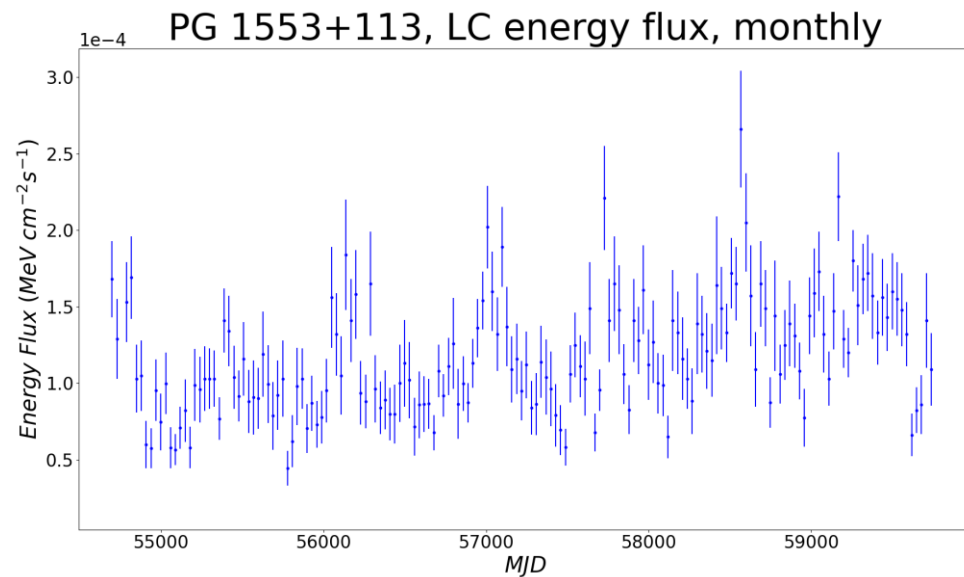


<sup>1</sup> <https://fermi.gsfc.nasa.gov/ssc/data/access/lat/LightCurveRepository/>

# Analysis

## Weighted Wavelet Z-transform (WWZ)

**Time series projection** onto a model function (**Morlet**) [5], to detects transient periodicities, studies temporal evolution of data and signal parameters.

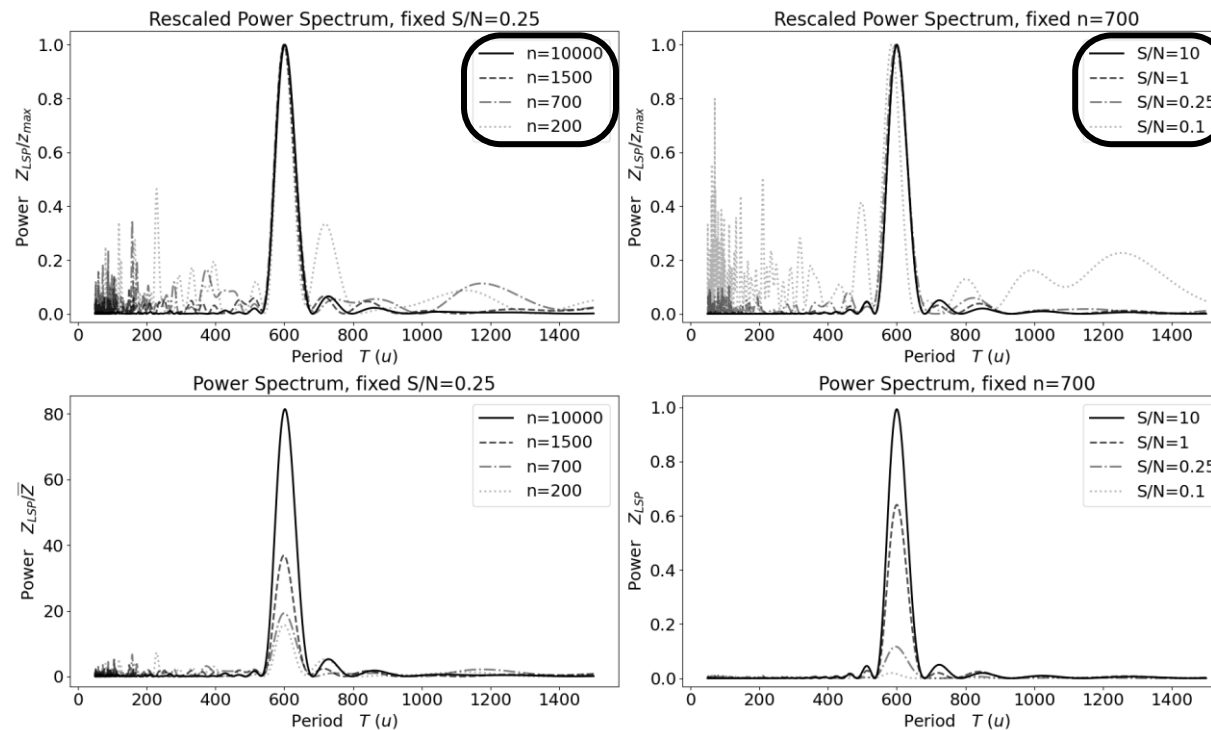


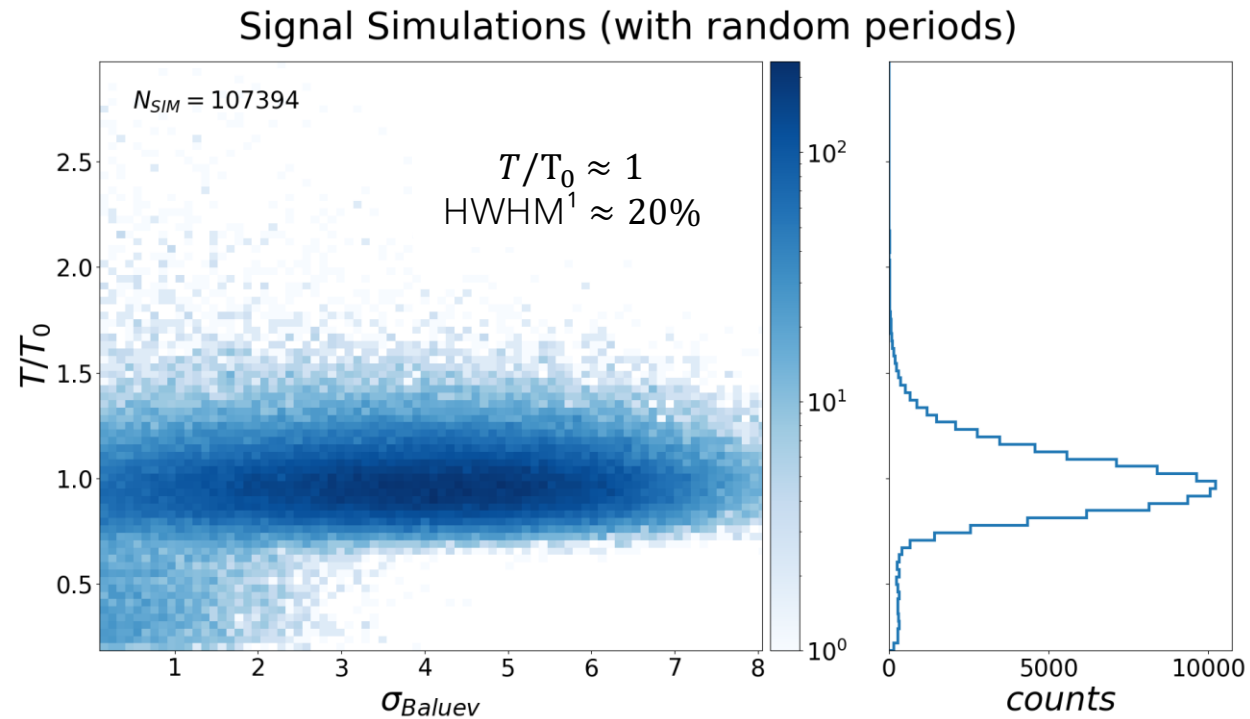
# Analysis

## Lomb-Scargle Periodogram (LSP)

**Square module of the Discrete Fourier transform.** In addition to the changes by Scargle [6] we take into account some consideration by Vanderplas [7].

The number of points  $n$  and the signal-to-noise ratio  $S/N$  do not affect the width of the peak but only its **height**.





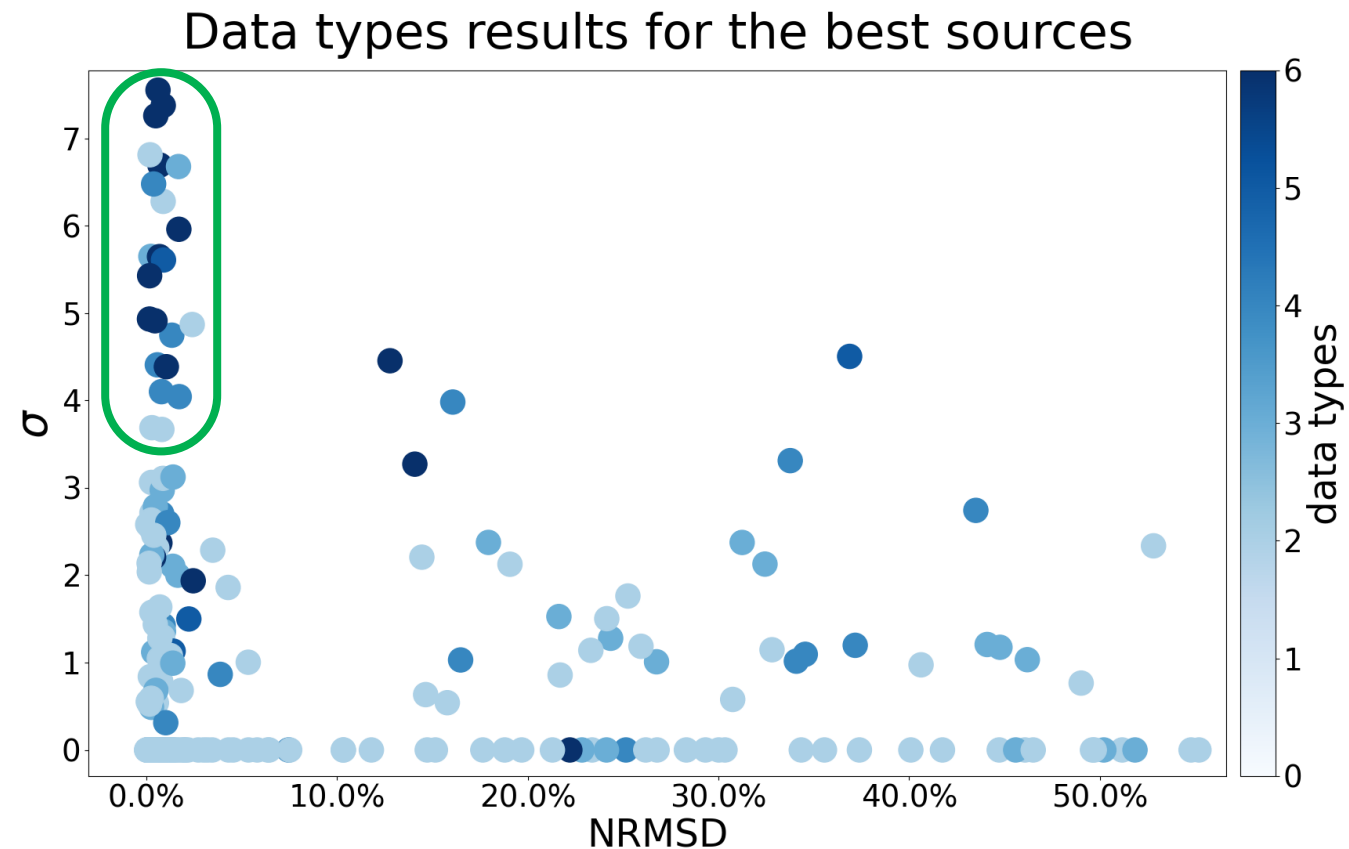
Preliminary significance estimation with **False Alarm Probability** (FAP) [7], comparing peak height with white noise background.

<sup>1</sup> Half Width at Half Maximum

# Analysis

## First Results from the Repository

Significant periodicities found in **23 blazars**. Many data types,  $> 3\sigma$ , and  $\text{NRMSD}^1 < 3\%$ . Cutoff 40% UL.



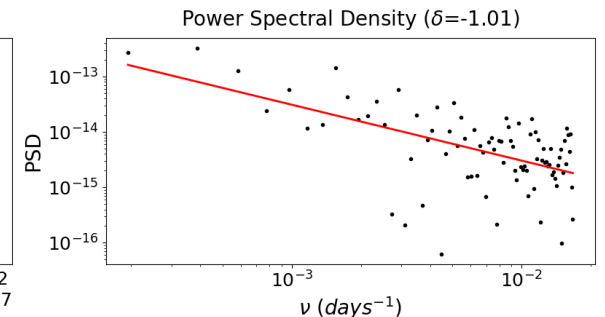
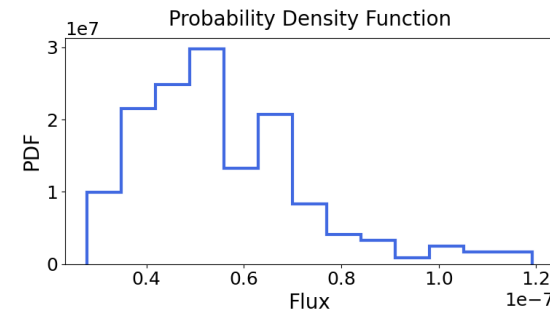
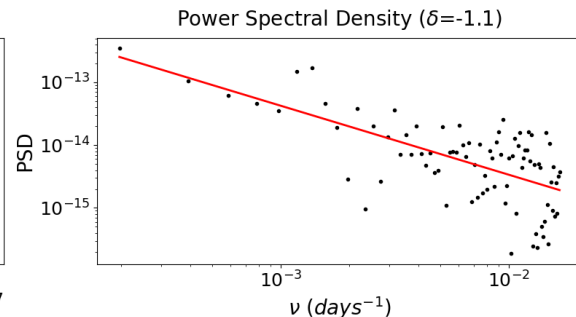
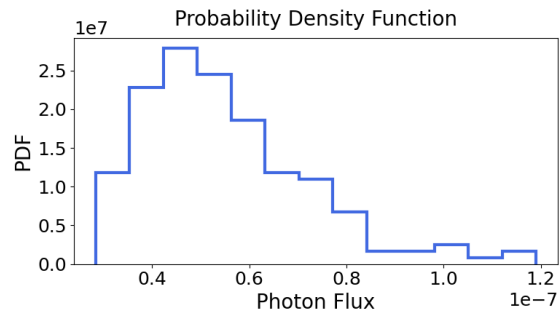
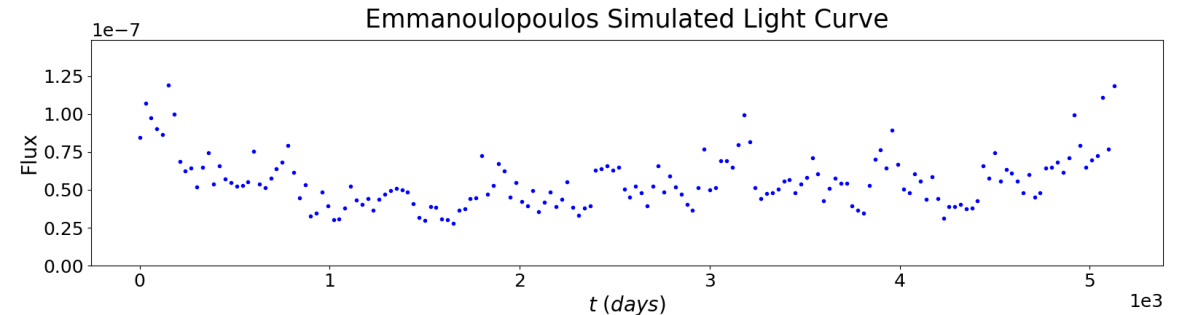
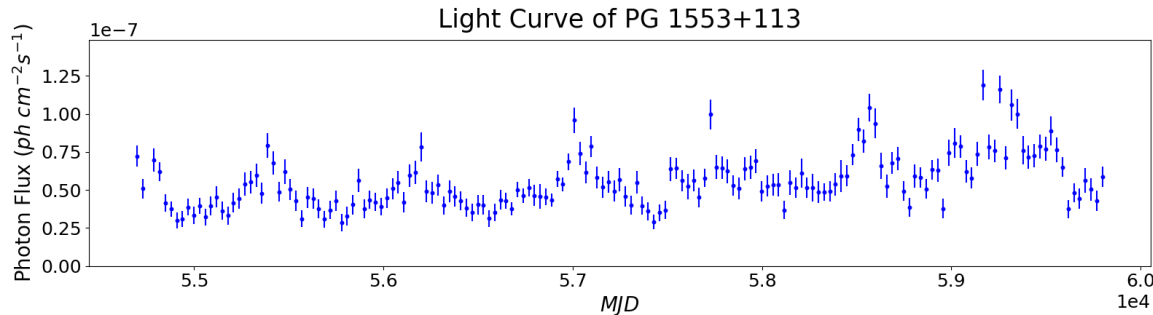
<sup>1</sup> Normalized Root Mean Square Deviation



# Analysis

## Emmanoulopoulos Simulations

Simulations with the Emmanoulopoulos algorithm [8] to study light curves with similar characteristics (**P**robability **D**ensity **F**unction and **P**ower **S**pectral **D**ensity).

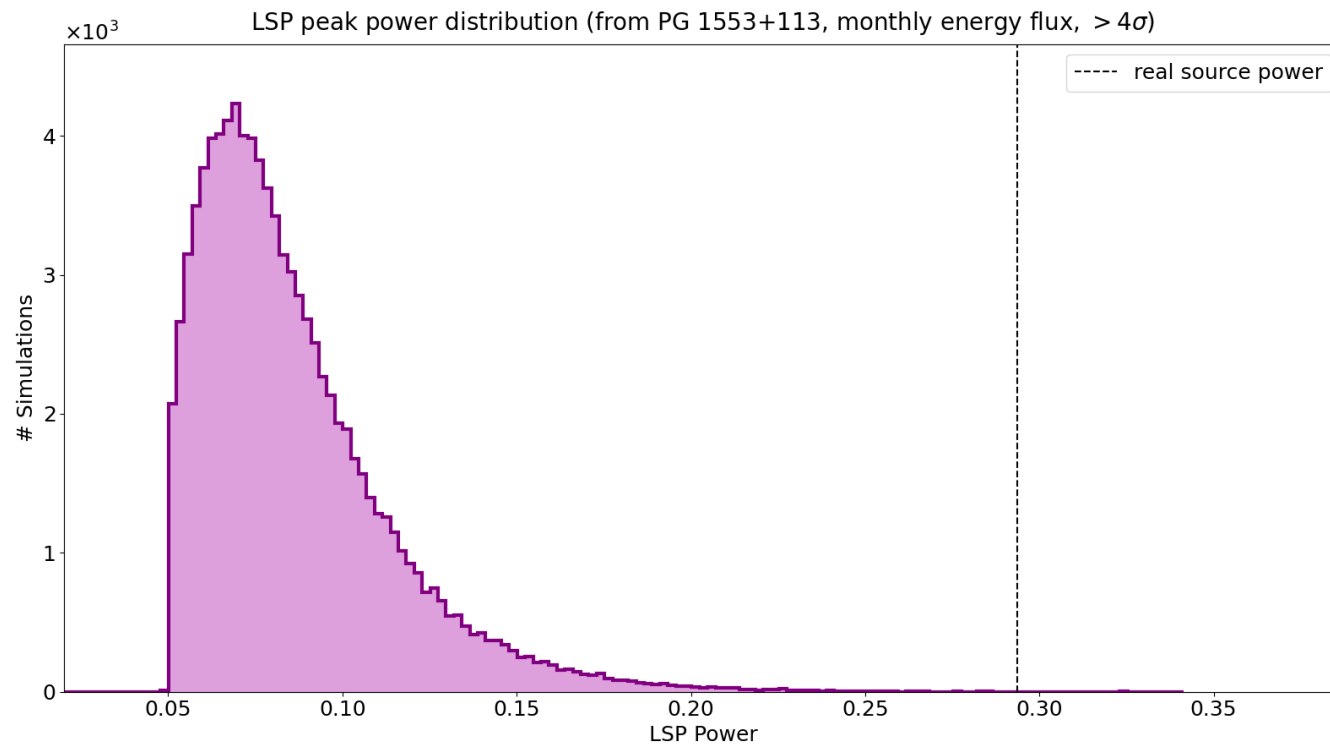


# Analysis

## Best Results and Golden Sample

Selected a subsample, for each source (and each sampling and flux type) we perform **1 000 000 simulations**.

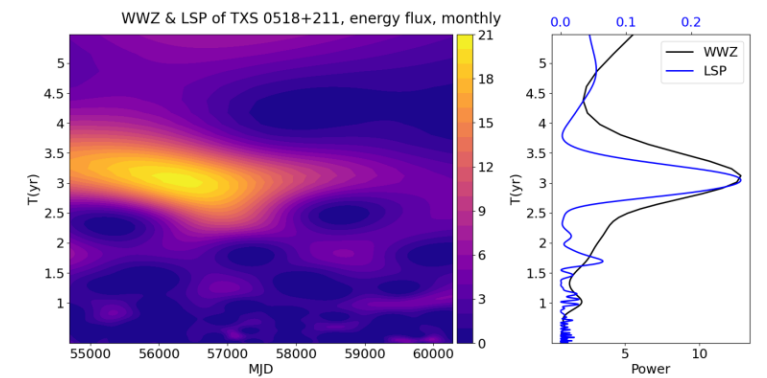
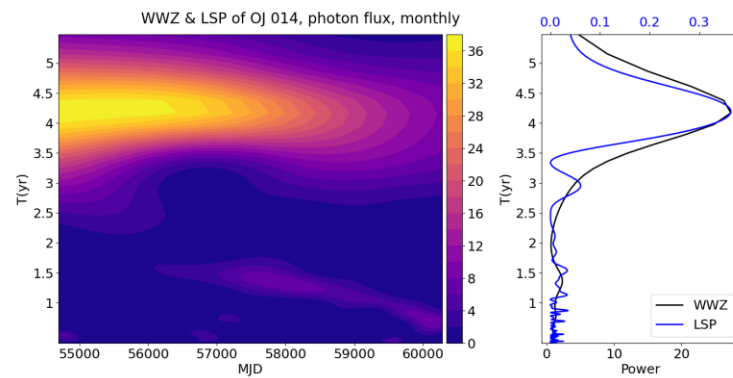
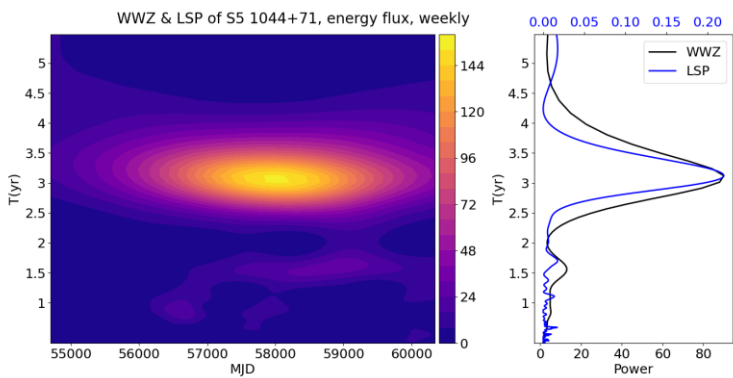
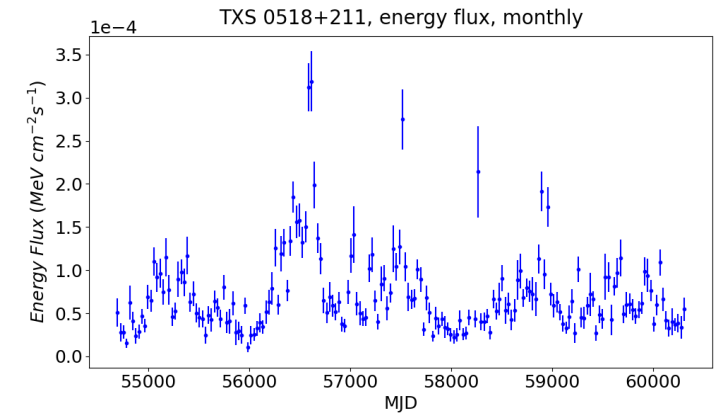
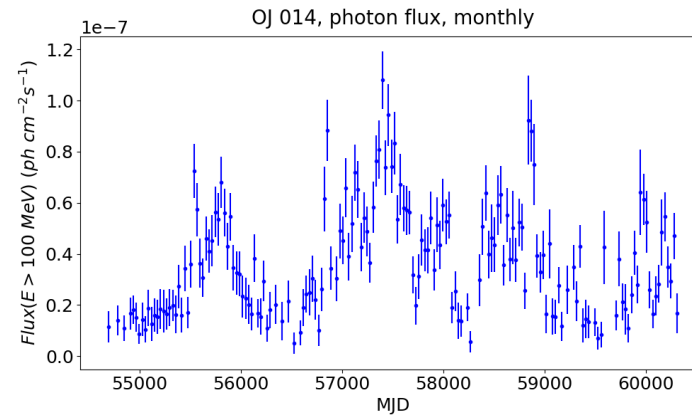
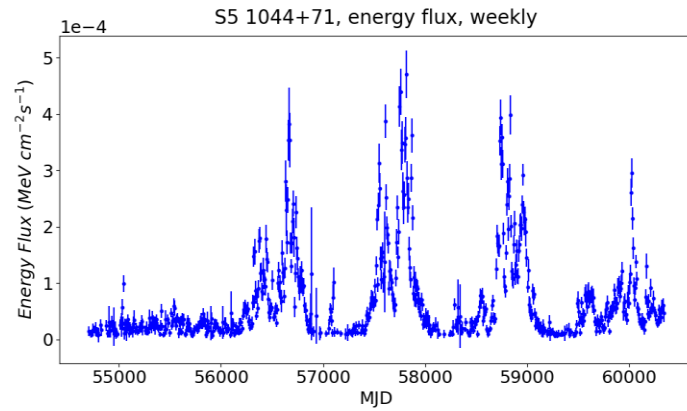
The *significance* is given by the number of times higher peak values are found in the LSP of the simulations.



Source Name	P (yr)	$N\sigma$
TXS 0059+581	4.2	$3.4\sigma$
MG1 J021114+1051	4.0	$2.7\sigma$
PKS 0215+015	3.4	$2.1\sigma$
PKS 0405-385	2.6	$2.2\sigma$
PKS 0426-380	3.7	$2.9\sigma$
PKS 0454-234	3.4	$3.0\sigma$
TXS 0518+211	3.0	$4.3\sigma$
S5 0716+71	2.4	$1.4\sigma$
OJ 014	4.1	$> 4.7\sigma$
S4 0814+42	2.2	$4.1\sigma$
S5 1044+71	3.1	$> 4.7\sigma$
S4 1144+40	3.3	$> 4.7\sigma$
B2 1215+30	2.8	$3.0\sigma$
4C +21.35	3.7	$1.8\sigma$
PG 1553+113	2.1	$> 4.7\sigma$
PKS 2155-304	1.6	$1.5\sigma$

# Analysis

## Best Results and Golden Sample



# Machine Learning

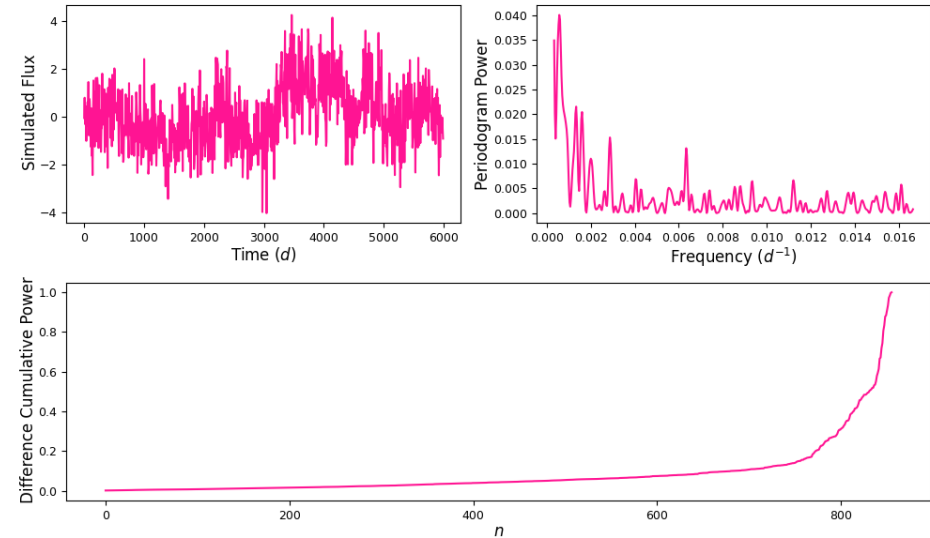
**t-Stochastic Neural Embedded** neighbor algorithm unsupervised [9] (**t-SNE**):

Calculates the probability that each high vectors  $\{x_j\}$  should be consider a neighbor of  $\{x_i\}$  from the set of Euclidean distances  $\{|\vec{x}_j - \vec{x}_i|\}$ .

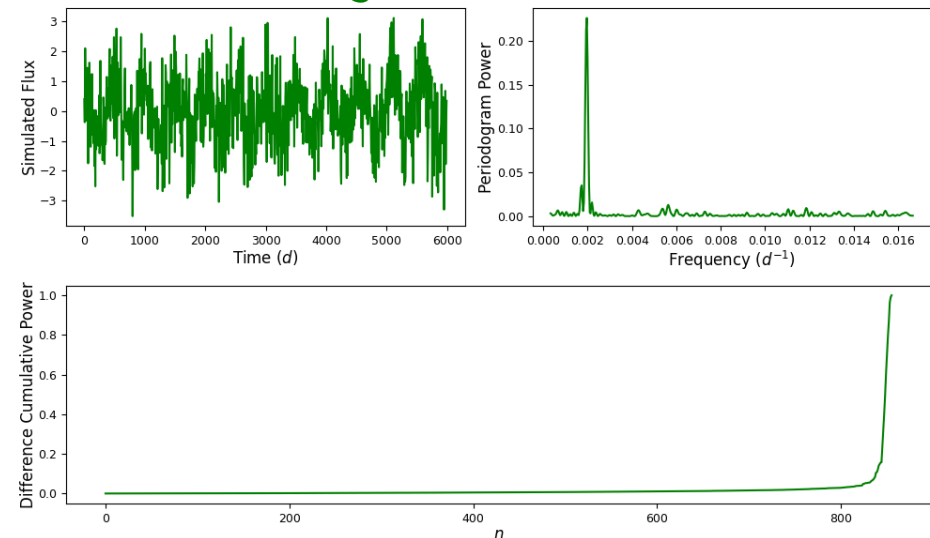
Since the vectors  $\{x\}$  are compared point to point we opted for the normalized **Difference Cumulative** of the sorted periodogram **Power**.

LSP power  $\rightarrow$  sort  $\rightarrow$  cumulative  $\rightarrow$   
 $\rightarrow$  difference  $(a_{i+1} - a_i) \rightarrow$  normalize

Pink / Red Noise Simulation



Signal Simulation



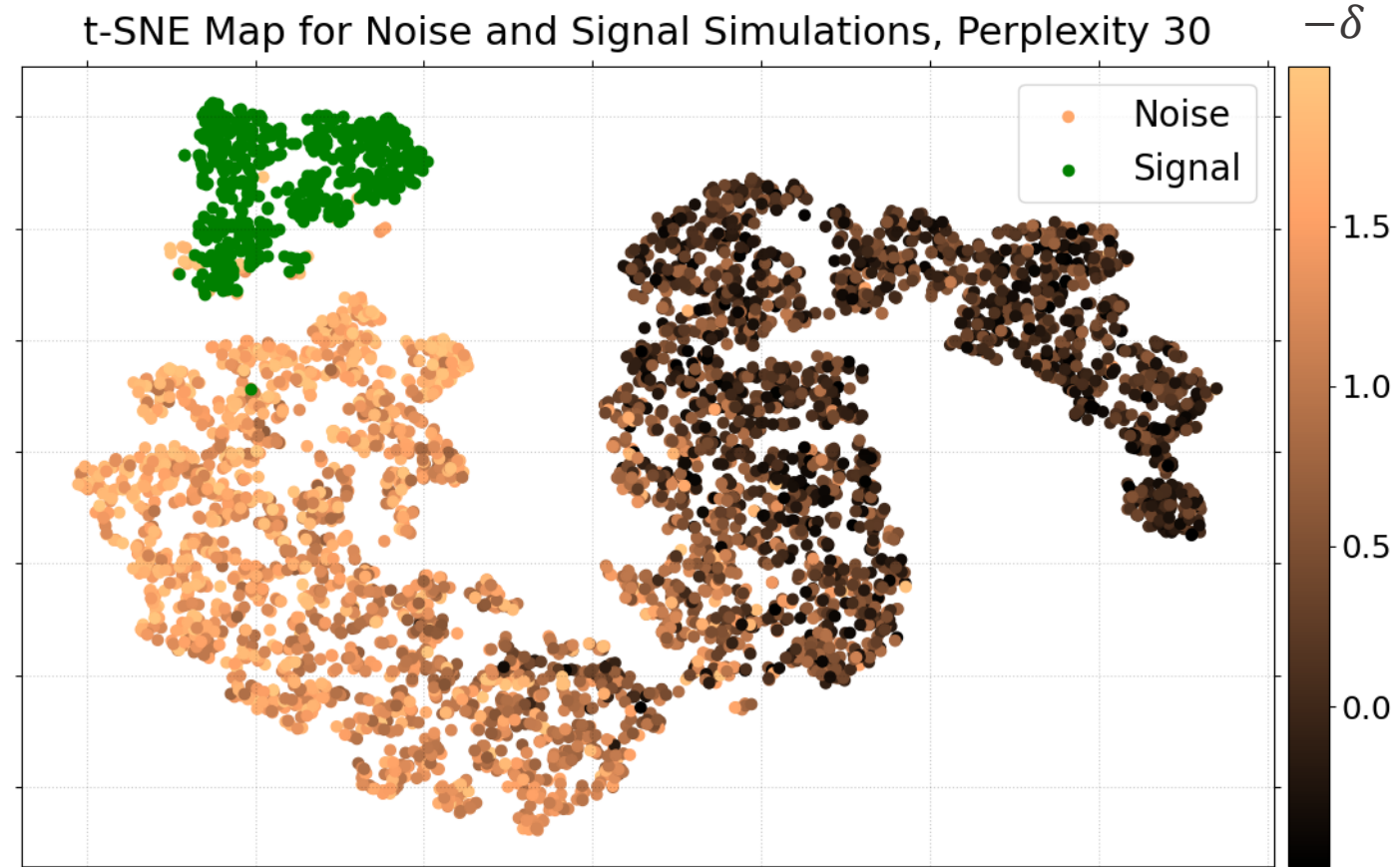
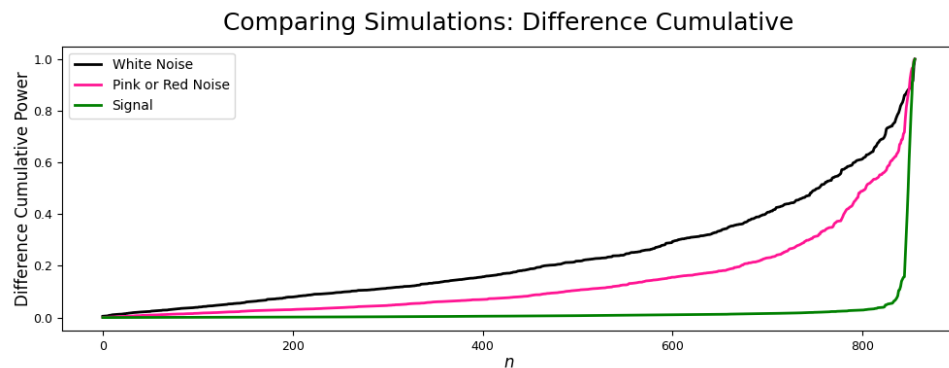
# Machine Learning

**t-SNE** produces a simplified map where the axes of this 2D space have no proper labels or meaning.

With this type of input the simulations can be distinguished.

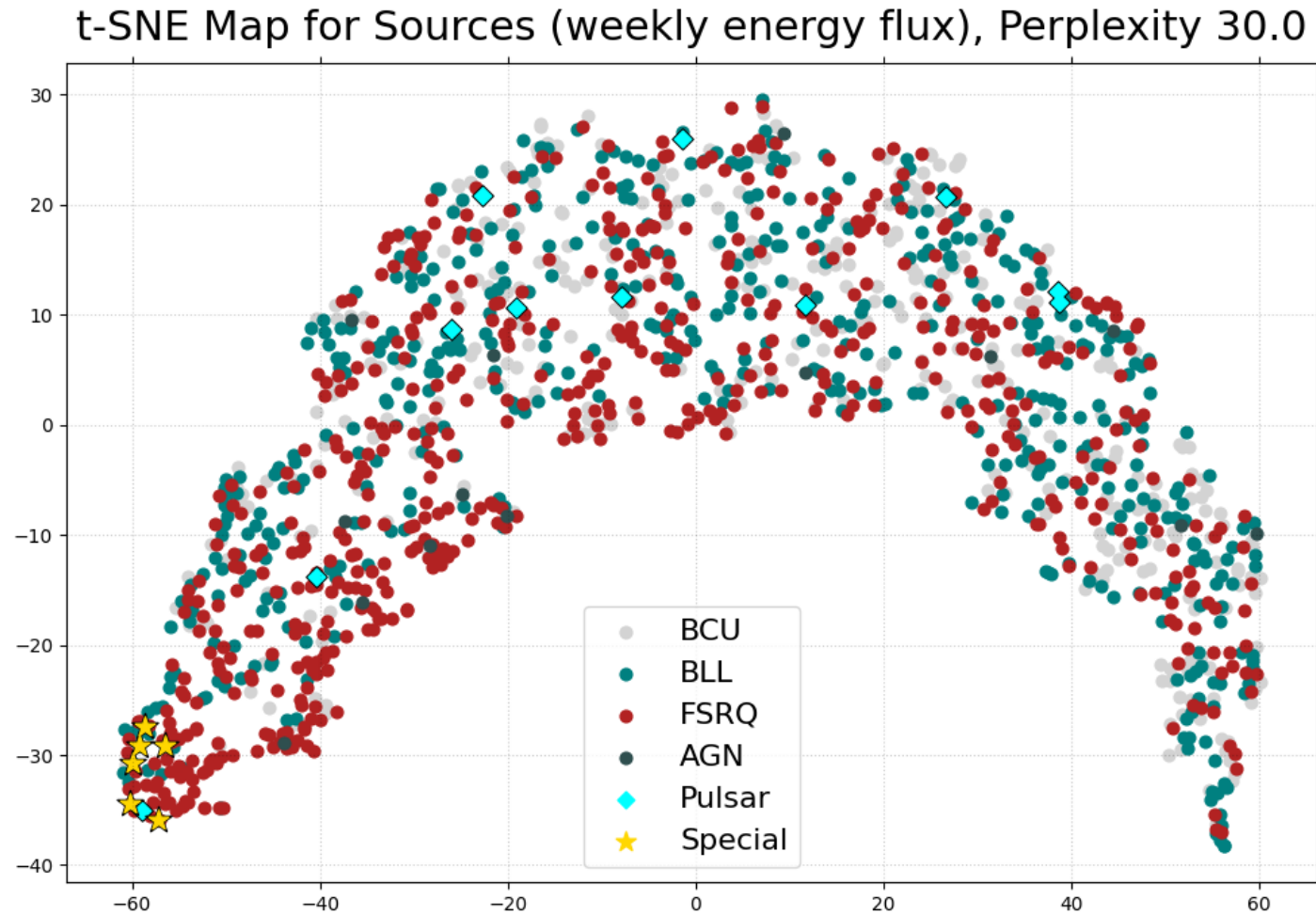
Characteristics of the simulations:

$$\text{SNR} = 1, -2.0 < \delta_{\text{noise}} < +0.5$$





# Machine Learning



With the sources around 60 of them are clustered near the **golden sample**.

# Outlook

---

- Periodicities in 1% (*similar sources in a previous work of Peñil et al. [2]*) of variable sources with 16 years data from LCR, and a **golden sample of 6 sources**.
- **t-SNE** method seems to bring out a larger cluster, but not separated enough.
- Increase the complexity of noise and signal simulation to obtain similar morphology in the map and try adding different types of **input data** (also multiwavelength).
- We do not exclude other machine learning methods, that may be better suited to the data and the goal.

# Outlook

---

- Periodicities in 1% (*similar sources in a previous work of Peñil et al. [2]*) of variable sources with 16 years data from LCR, and a **golden sample of 6 sources**.
- **t-SNE** method seems to bring out a larger cluster, but not separated enough.
- Increase the complexity of noise and signal simulation to obtain similar morphology in the map and try adding different types of **input data** (also multiwavelength).
- We do not exclude other machine learning methods, that may be better suited to the data and the goal.



?!

# Outlook

---

- Periodicities in 1% (*similar sources in a previous work of Peñil et al. [2]*) of variable sources with 16 years data from LCR, and a **golden sample of 6 sources**.
  - **t-SNE** method seems to bring out a larger cluster, but not separated enough.
  - Increase the complexity of noise and signal simulation to obtain similar morphology in the map and try adding different types of **input data** (also multiwavelength).
  - We do not exclude other machine learning methods, that may be better suited to the data and the goal.
- Comparing spectral models with a Bayesian approach for the golden sample for a more robust analysis.

New outlook  
(more work)  
thanks to Fermi  
Summer School

# Bibliography

---

- [1] M. Ackermann, et al., "*Multiwavelength evidence for quasi-periodic modulation in the gamma-ray blazar pg 1553+113*", The Astrophysical Journal, vol. 813, p. L41, Nov 2015.
- [2] P. Peñil, et al., "*Systematic Search for  $\gamma$ -Ray Periodicity in Active Galactic Nuclei Detected by the Fermi Large Area Telescope*", ApJ, vol. 896, p. 134, June 2020.
- [3] S. Komossa, "*Observational evidence for binary black holes and active double nuclei*", Memorie della Società Astronomica Italiana, vol. 77, p. 733, 2006.
- [4] M. Tavani, Marco, et al. "*The blazar PG 1553+ 113 as a binary system of supermassive black holes*", ApJ 854.1 (2018): 11.
- [5] G. Foster, "*Wavelets for period analysis of unevenly sampled time series*", AJ, vol. 112, pp. 1709-1729, Oct. 1996.
- [6] J. D. Scargle, "*Studies in astronomical time series analysis. II. Statistical aspects of spectral analysis of unevenly spaced data*", ApJ, vol. 263, pp. 835-853, Dec. 1982.
- [7] J. T. VanderPlas, "*Understanding the Lomb-Scargle Periodogram*", ApJS, vol. 236, p. 16, May 2018.
- [8] D. Emmanoulopoulos, I. M. McHardy, and I. E. Papadakis. "*Generating artificial light curves: revisited and updated.*" Monthly Notices of the Royal Astronomical Society 433.2 (2013): 907-927.
- [9] L. van der Maaten and G. Hinton, "*Visualizing Data using t-SNE*", Journal of Machine Learning Research 9 (86), 2579-2605, 2008.



# ***Backup Slides***

# Weighted Wavelet Z-transform (WWZ)

**Time series projection** onto a model function (**Morlet**) [3].

$$W = \sum_k^N x(t_k) F^*(t_k)$$

With the S-matrix  $S_{ab} = \langle F_a | F_b \rangle$  as our metric tensor with statistical weights  $w$  in it, then the inner product of two function is:

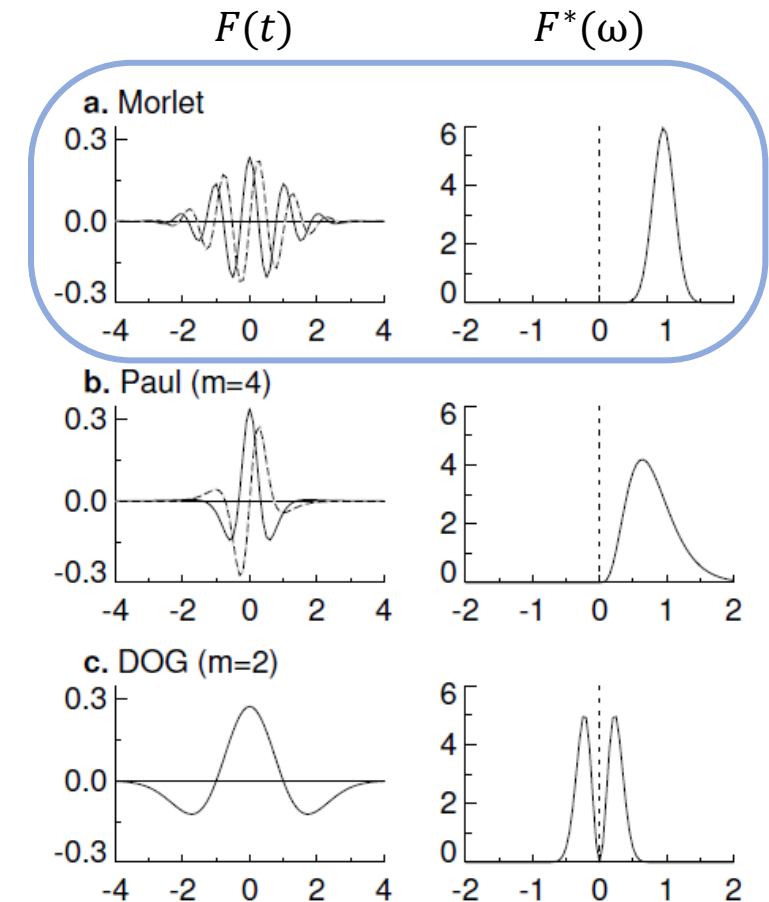
$$\langle f | g \rangle = \sum_a \sum_b S_{ab} f_a g_b$$

Hence, using the variations  $V_x = \langle x | x \rangle - \langle 1 | x \rangle^2$  and  $V_R = \langle R | R \rangle - \langle 1 | R \rangle^2$  where the first is variations of the data and the second of the residual vector.

The WWZ is defined as:

$$Z = \frac{(N_{eff} - 3)V_R}{2(V_x - V_R)}$$

Where  $N_{eff} = (\sum w_\alpha)^2 / \sum w_\alpha^2$ .



[https://doi.org/10.1175/1520-0477\(1998\)079<0061:APGTWA>2.0.CO;2](https://doi.org/10.1175/1520-0477(1998)079<0061:APGTWA>2.0.CO;2)

# Lomb-Scargle Periodogram (LSP)

**Square module of the Discrete Fourier transform.** In addition to the changes by Scargle [4] we take into account some consideration by Vanderplas [5].

Signal and noise:  $x_j = x(t_j) = x_s j + r_j$     Classic periodogram:  $P_x(\omega) = \frac{1}{N} |DFT_x(\omega)|^2 = \frac{1}{N} |\sum_{j=1}^N x(t_j) e^{-i\omega t_j}|^2$

Not useful in case of noisy data. Spectral Leakage.

Discrete Fourier Transform:

$$DFT_x(\omega) = \sqrt{N/2} \sum_{j=1}^N x(t_j) (A(\omega) \cos \omega t_j + iB(\omega) \sin \omega t_j)$$

If  $A(\omega) = B(\omega) = \sqrt{2/N}$  we obtain the classic periodogram. Lomb-Scargle changes:

$$A(\omega) = \left( \sum_j \cos^2 \omega t_j \right)^{-1/2} ; \quad B(\omega) = \left( \sum_j \sin^2 \omega t_j \right)^{-1/2}$$

Modified periodogram:

$$P_x(\omega) = \frac{1}{2} \left( \frac{(\sum_j x_j \cos \omega(t_j - \tau))^2}{\sum_j x_j \cos^2 \omega(t_j - \tau)} + \frac{(\sum_j x_j \sin \omega(t_j - \tau))^2}{\sum_j x_j \sin^2 \omega(t_j - \tau)} \right) \quad \text{with} \quad \tan 2\omega\tau = \frac{\sum_j \sin 2\omega t_j}{\sum_j \cos 2\omega t_j}$$

# False Alarm Probability (FAP)

---

To compare **peak height** with **background** and **spurious peaks**.

Probability that a peak of a certain height  $Z$  will be found from a data set consisting of white noise.

## ❖ Naive

The cumulative probability of observing a value less than  $Z$  with white noise is  $P(Z) = 1 - e^{-Z}$ .

$$FAP_{Naive}(Z) = 1 - (P(Z))^{N_{eff}}$$

## ❖ Bootstrap

Randomization of the time series, high computational cost. Simulations required:  $N=10/r$ , for a false positive rate  $r$ .

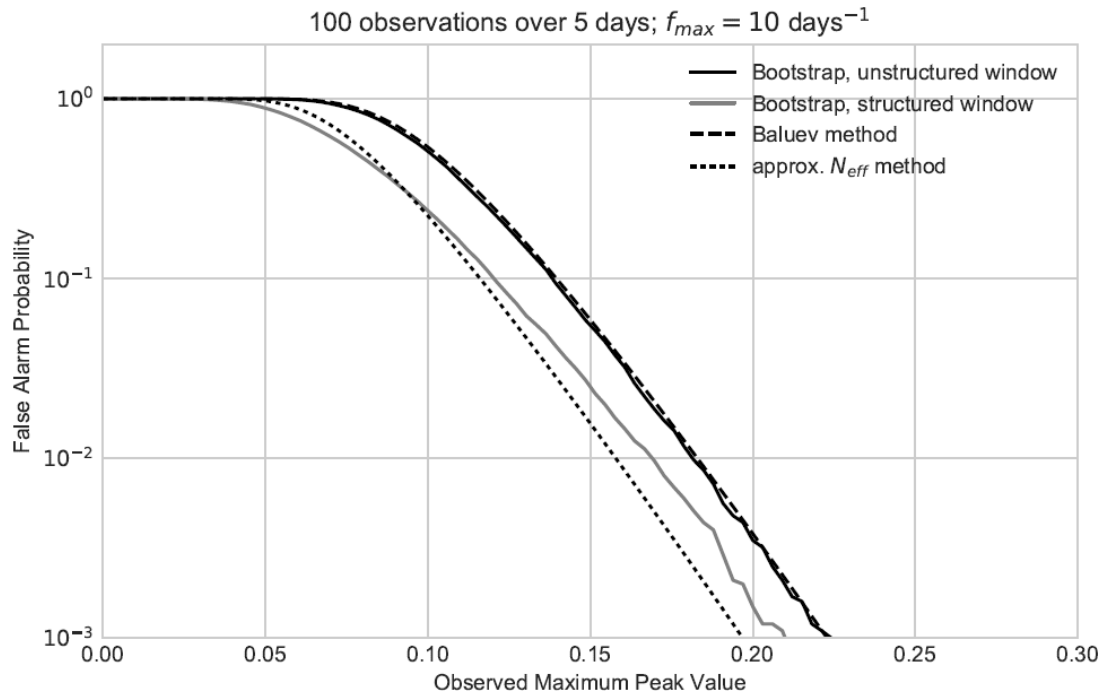
## ❖ Baluev

Extreme value theory for random processes. Upperbound for the FAP.

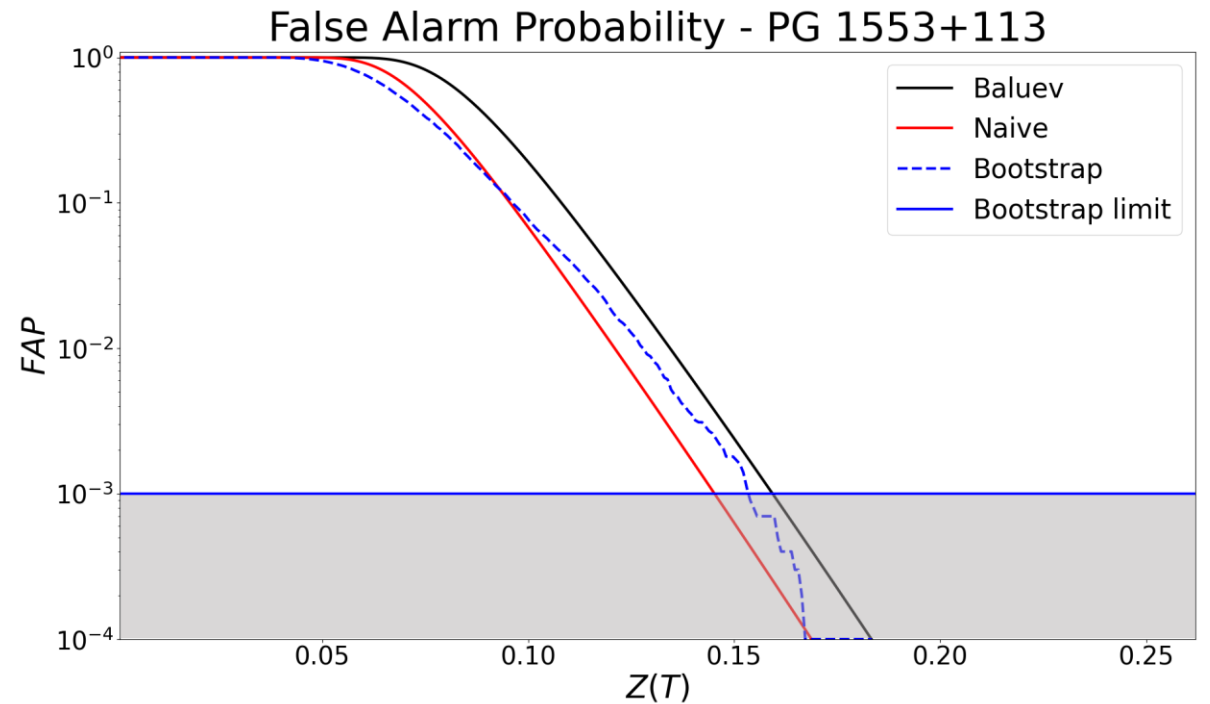
# False Alarm Probability (FAP)

**Bootstrap** is the most reliable method, **Naive** overestimates the significance, while **Baluev** underestimates it.

From the FAP we extrapolate a fictitious number of  $\sigma$ .



From Vanderplas, 2016 [5]





# Baluev FAP

---

Two hypothesis: noise H and periodic signal K. FAP comes from the probability distribution of maxima in periodograms under H hypothesis.

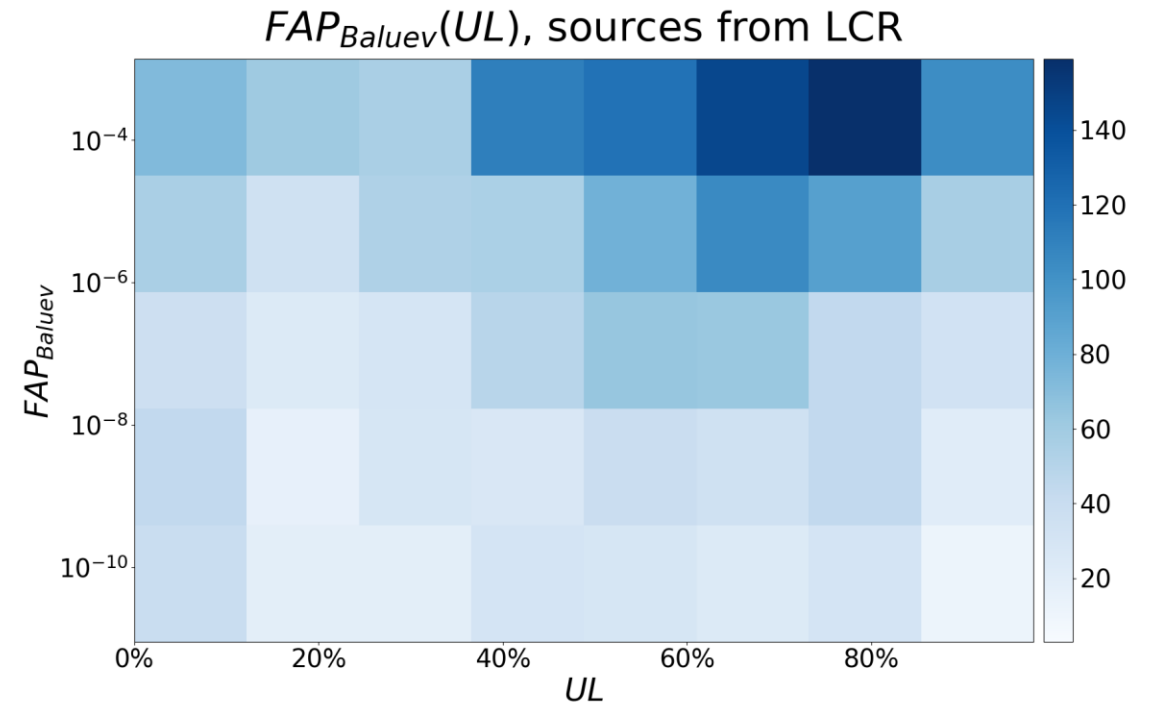
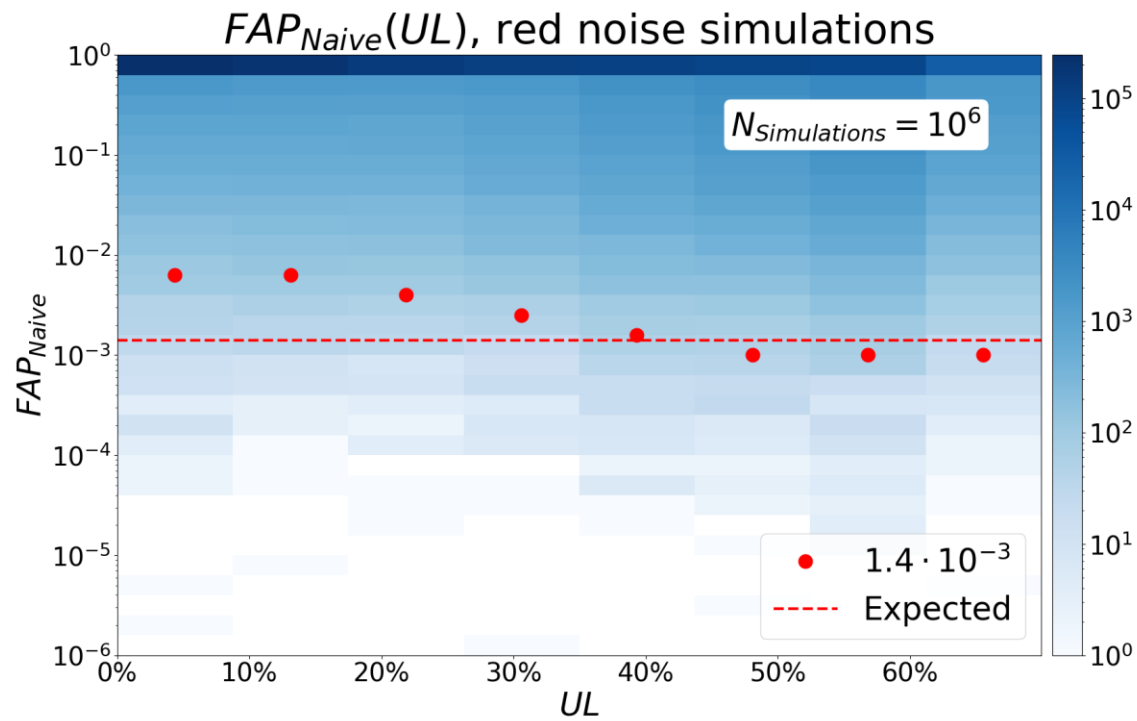
Least-squares periodogram:

$$z(f) = \frac{\chi_H^2 - \chi_K^2(f)}{2}$$

With the theory of random processes we estimate the FAP:

$$FAP_{Baluev}(z, f_{max}) = 1 - \exp(-W e^{-z} \sqrt{z})$$
$$W = f_{max} T_{eff} \quad ; \quad T_{eff} = \sqrt{4\pi Dt} \quad ; \quad Dt = \bar{t}^2 - \bar{t}^2$$

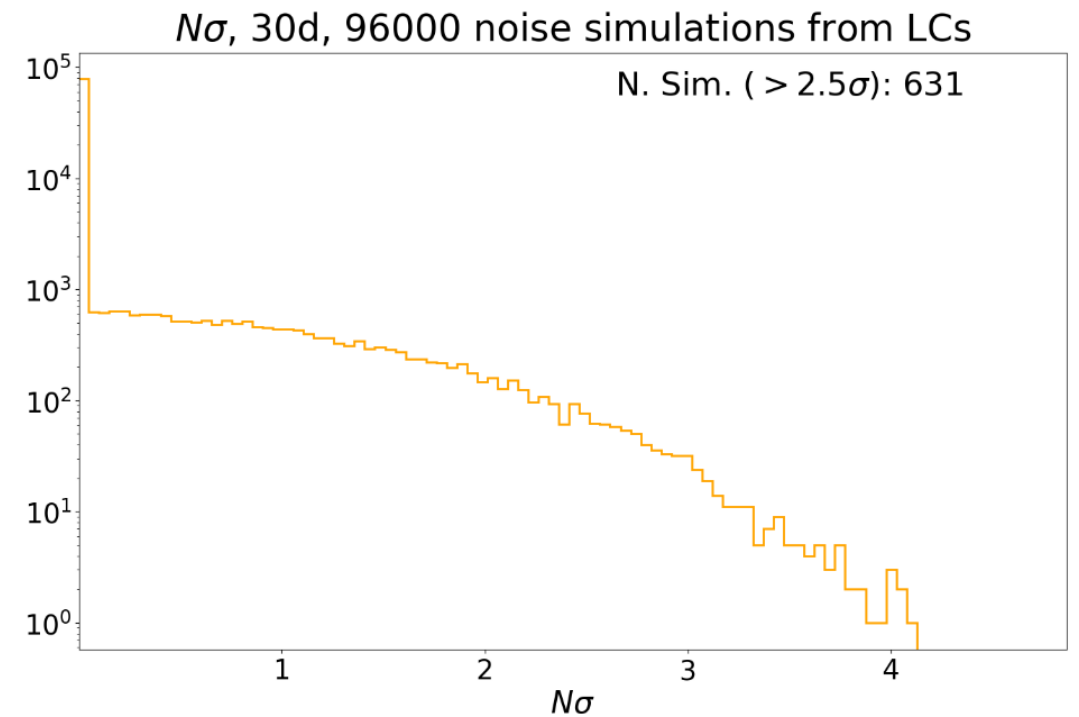
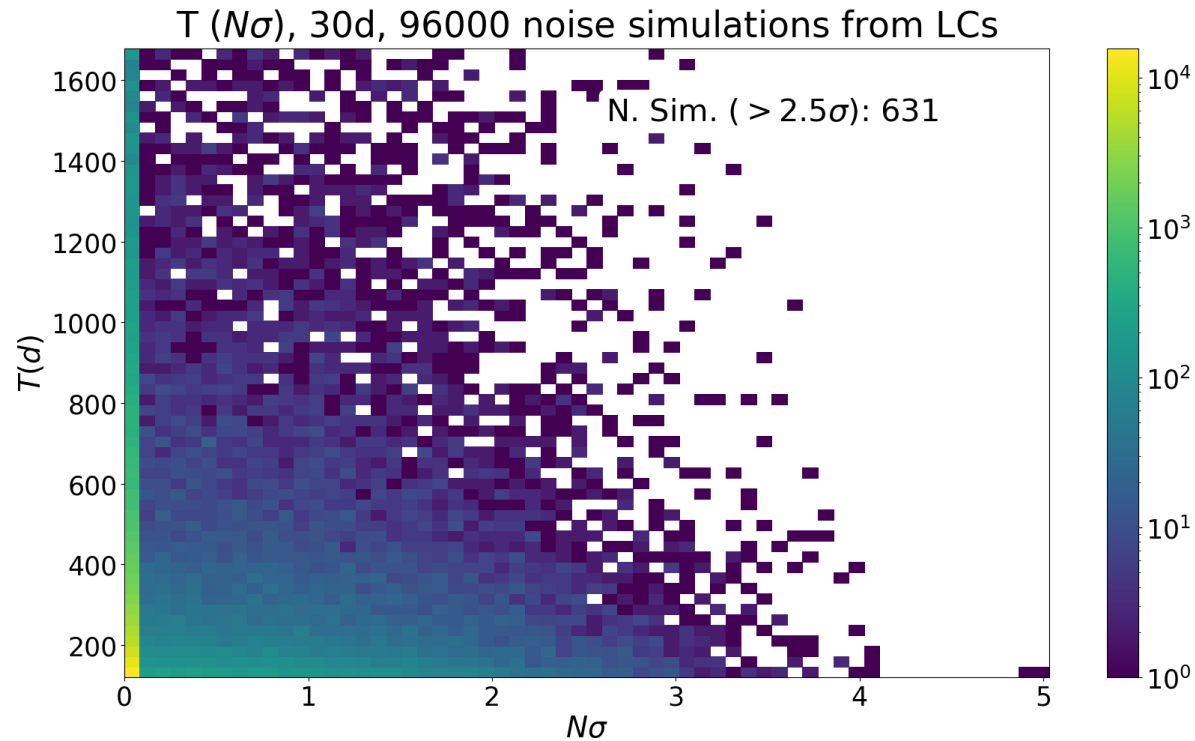
# False Alarm Probability (FAP)



# Time Series and Noise Simulations

**White Noise simulations** as uniform randomization of Blazar light curves.

A period with significance  $> 2.5\sigma$  is found in less than 1% simulations.



<sup>1</sup> Half Width at Half Maximum

# Emmanoulopoulos Simulations

---

Simulations with the Emmanoulopoulos algorithm [6] to study light curves with similar characteristics (Probability Density Function and Power Spectral Density).

## First step:

From the PSD make Timmer-König simulation:  $x_{TK}(t)$ , perform the DFT (Discrete Fourier Function) on it and take the amplitude  $A_{TK}$ .

## Second step:

Take  $x_0(t)$ , White Noise simulation obtained from the PDF, perform the DFT and take phase  $\phi_0$ .

## Third step:

Combine  $A_{TK}$  and  $\phi_0$  to have a  $X(j)$  in the frequency domain, perform the IDFT (Inverse) obtaining  $x_c(t)$ .

## Fourth step:

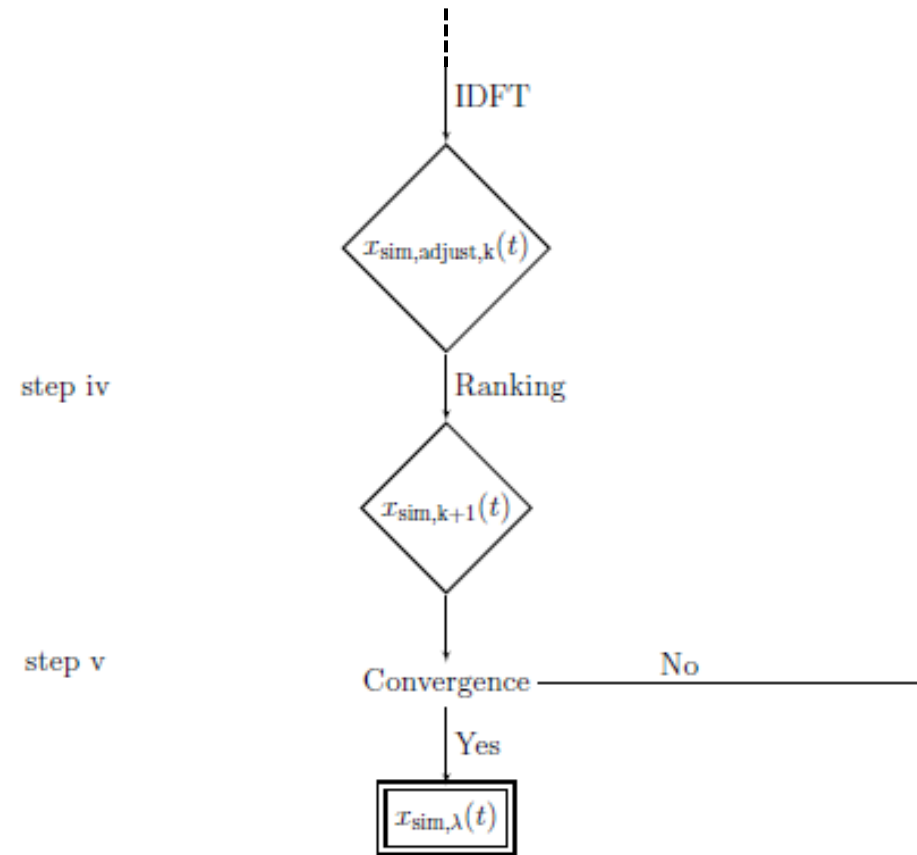
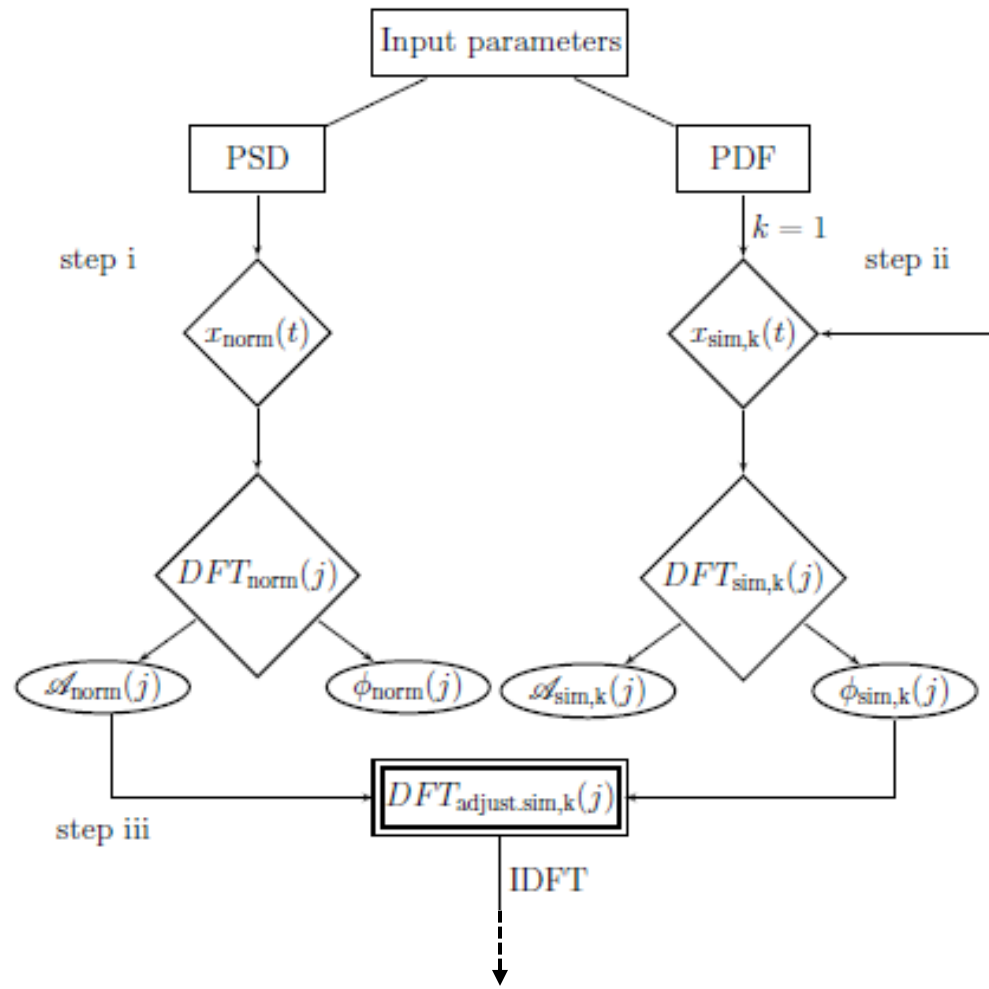
Sort  $x_c(t)$  in descending order and replace the values  $x_c$  with  $x_0$ , also sorted in descending order, obtaining  $x_i(t)$ , where  $i$  is the number of iterations.

## Fifth step:

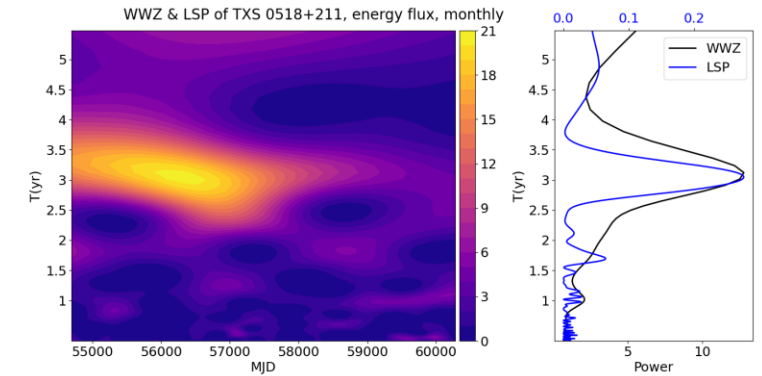
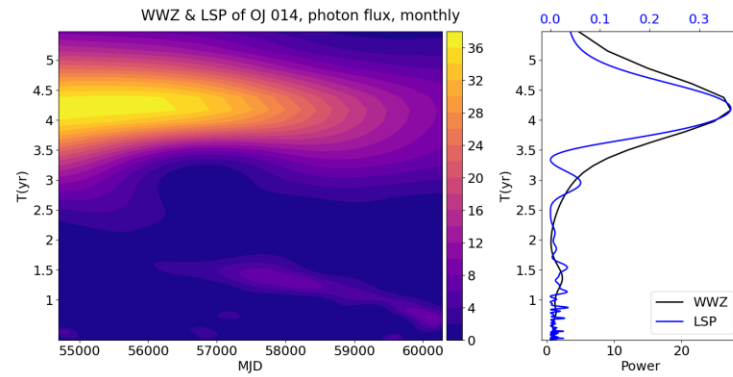
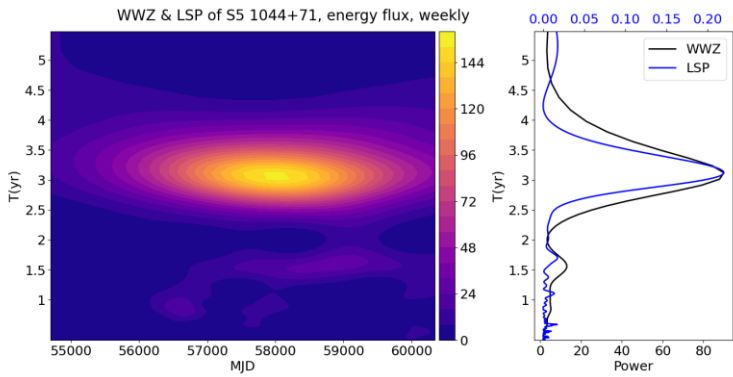
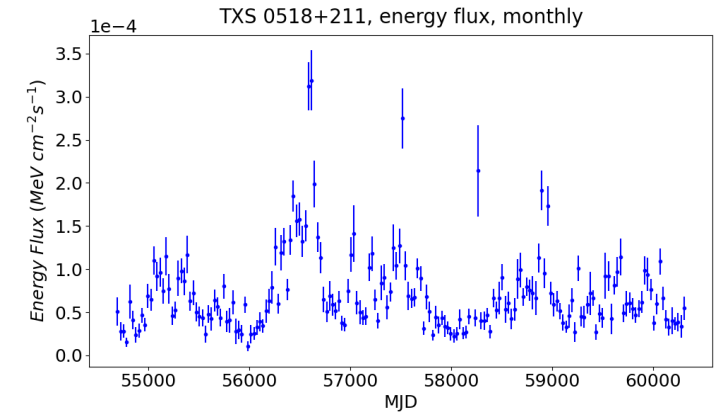
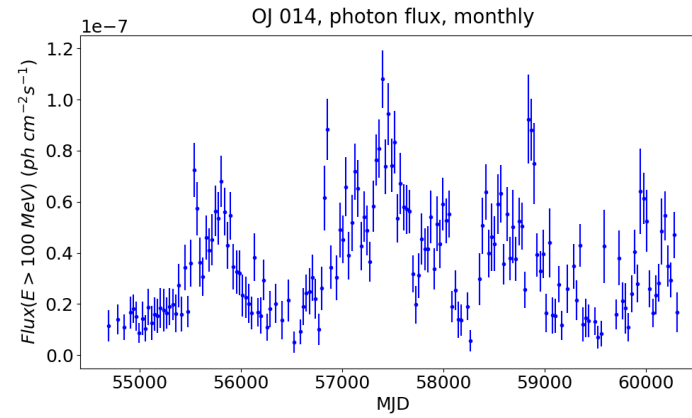
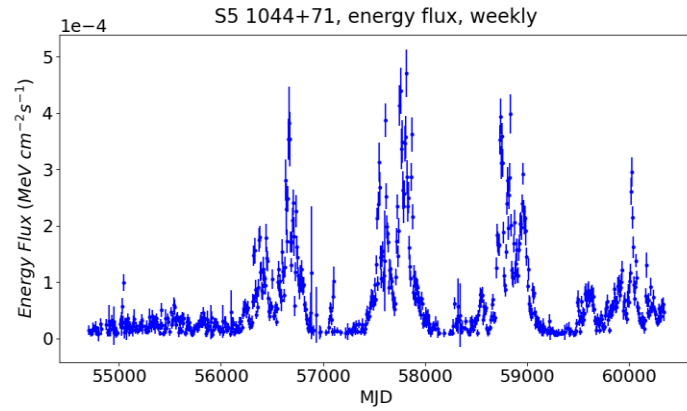
Replacing  $x_0(t)$  with the new  $x_i(t)$ , repeat the process from the second step until it converges i.e. when  $x_i(t)$  and  $x_{i-1}(t)$  have the same PSD.



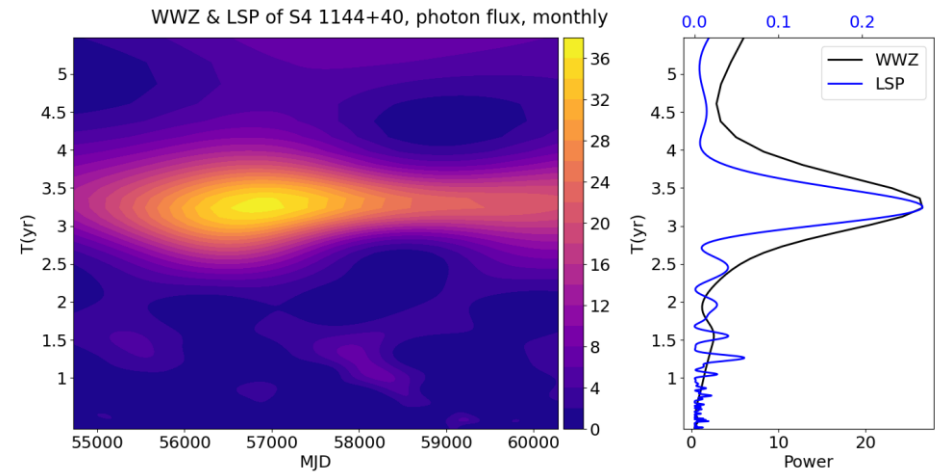
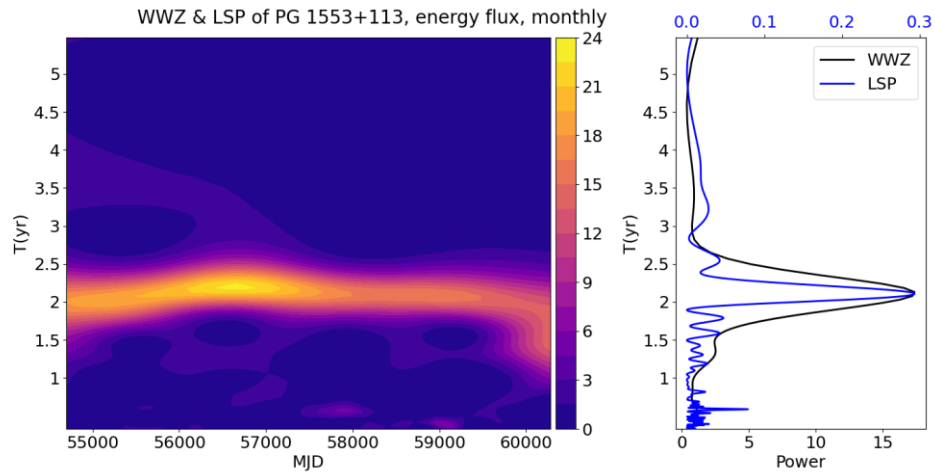
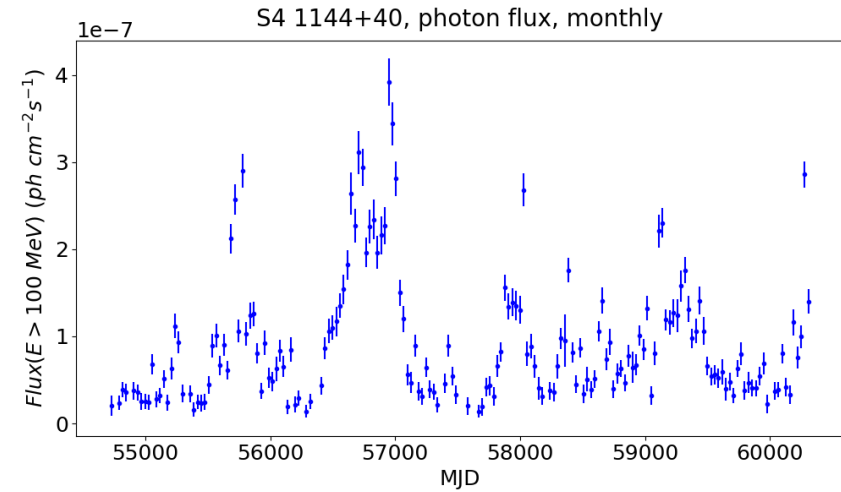
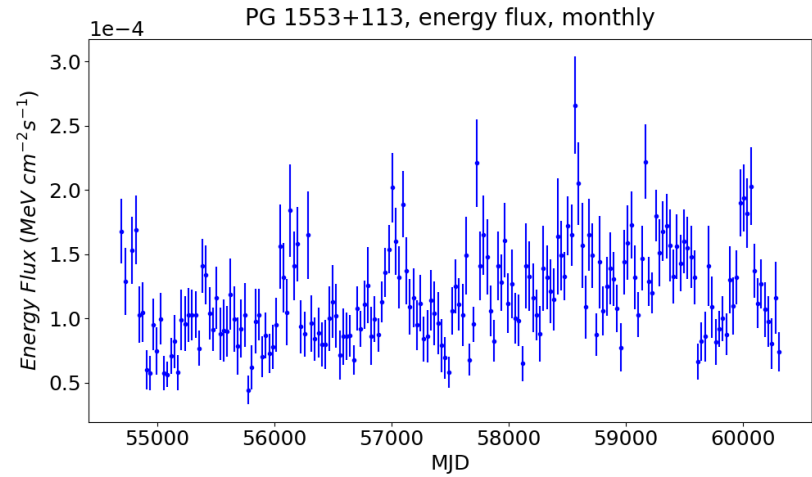
# Emmanoulopoulos Simulations



# Golden Sample

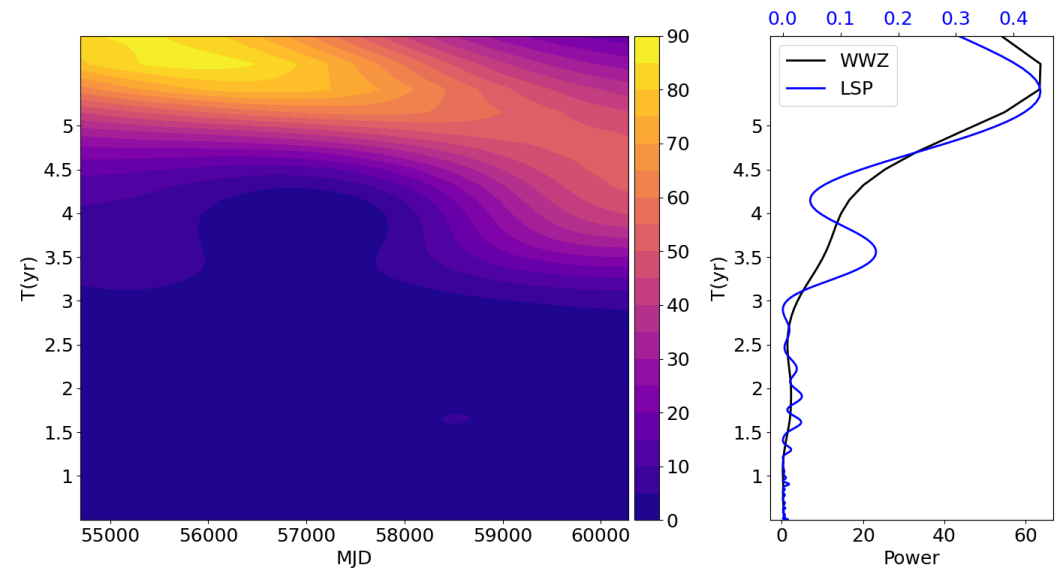
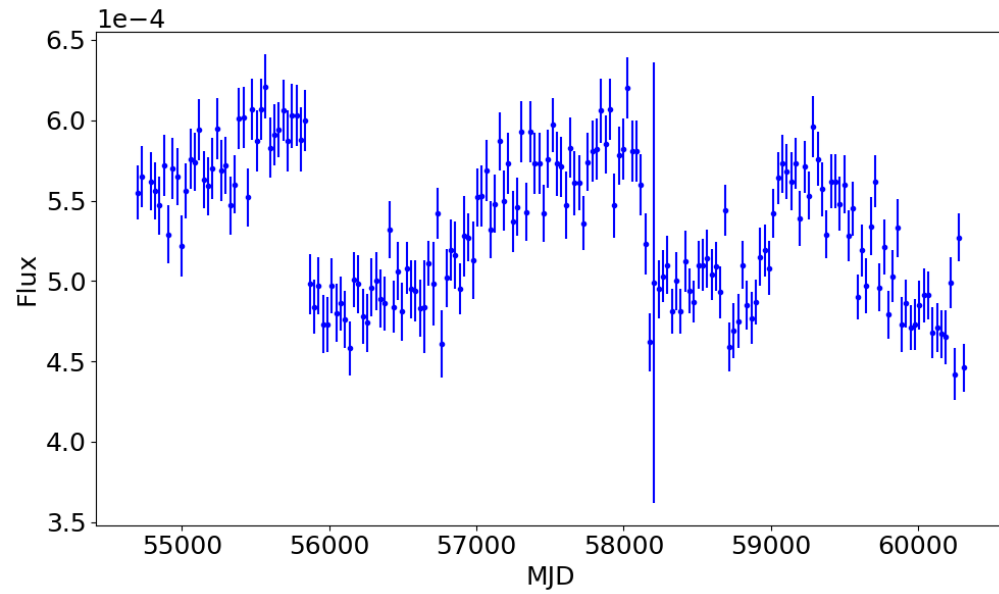


# Golden Sample





# Pulsar



# Look-elsewhere effect

---

Apparent statistically significant observation, which has arisen from searching a large parameter space.

The **Trial Factor (N)** is used to account this effect. It is the ratio between the probability of observing a possible excess at some fixed point, to the probability of observing it anywhere in the range.

The local significance is reduced to the global significance (local>global).

$$p_{GLOBAL} = 1 - (1 - p_{LOCAL})^N$$

In this case someone considers  $N = P \cdot B$ , where  $P$  is the number of independent periods and  $B$  is the number of blazars.

In a previous work on the catalog:  $N = 35 \cdot 351 = 12,285$ , so a local  $5.5 \sigma$  become  $2.8 \sigma$  global significance). While in a paper about PG 1553+113, is  $N = P \cdot 1 = 43$ .

# t-SNE, theory

---

---

**Algorithm 1:** Simple version of t-Distributed Stochastic Neighbor Embedding.

---

**Data:** data set  $\mathcal{X} = \{x_1, x_2, \dots, x_n\}$ ,

cost function parameters: perplexity  $Perp$ ,

optimization parameters: number of iterations  $T$ , learning rate  $\eta$ , momentum  $\alpha(t)$ .

**Result:** low-dimensional data representation  $\mathcal{Y}^{(T)} = \{y_1, y_2, \dots, y_n\}$ .

**begin**

    compute pairwise affinities  $p_{j|i}$  with perplexity  $Perp$  (using Equation 1)

    set  $p_{ij} = \frac{p_{j|i} + p_{i|j}}{2n}$

    sample initial solution  $\mathcal{Y}^{(0)} = \{y_1, y_2, \dots, y_n\}$  from  $\mathcal{N}(0, 10^{-4}I)$

**for**  $t=1$  **to**  $T$  **do**

        compute low-dimensional affinities  $q_{ij}$  (using Equation 4)

        compute gradient  $\frac{\delta C}{\delta \mathcal{Y}}$  (using Equation 5)

        set  $\mathcal{Y}^{(t)} = \mathcal{Y}^{(t-1)} + \eta \frac{\delta C}{\delta \mathcal{Y}} + \alpha(t) (\mathcal{Y}^{(t-1)} - \mathcal{Y}^{(t-2)})$

**end**

**end**

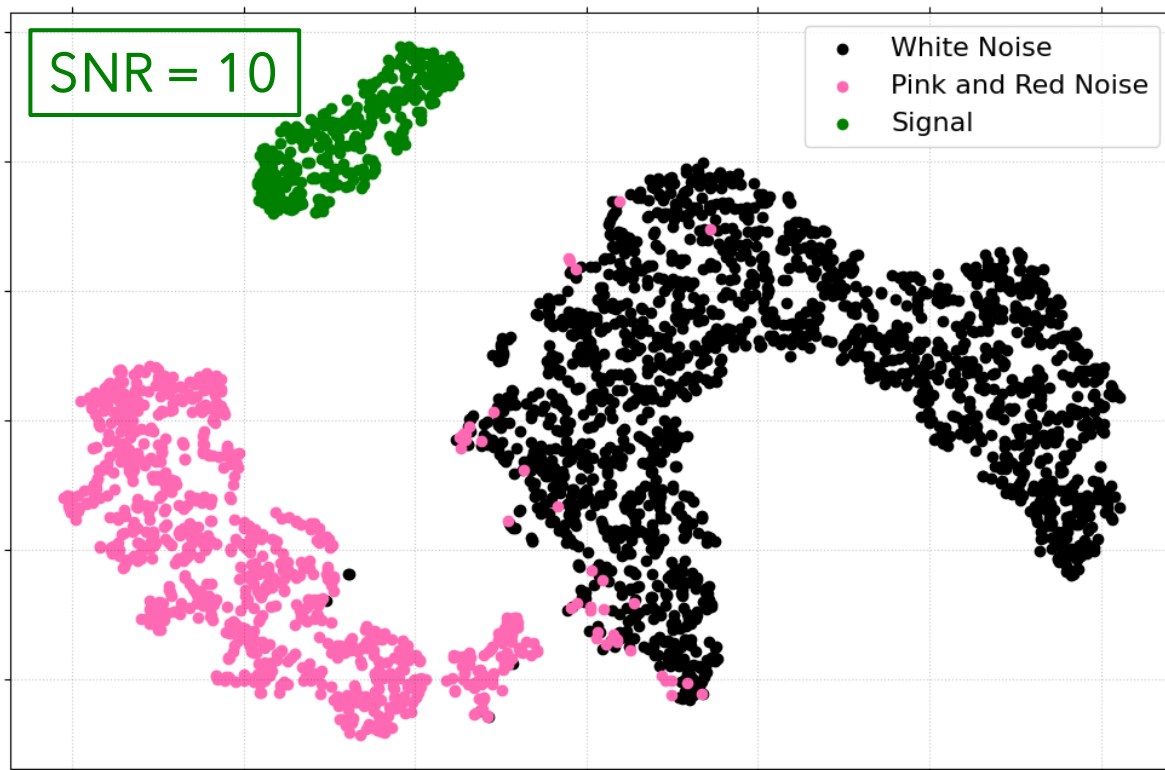
---

$$\epsilon(P_i) = 2^{H(P_i)},$$

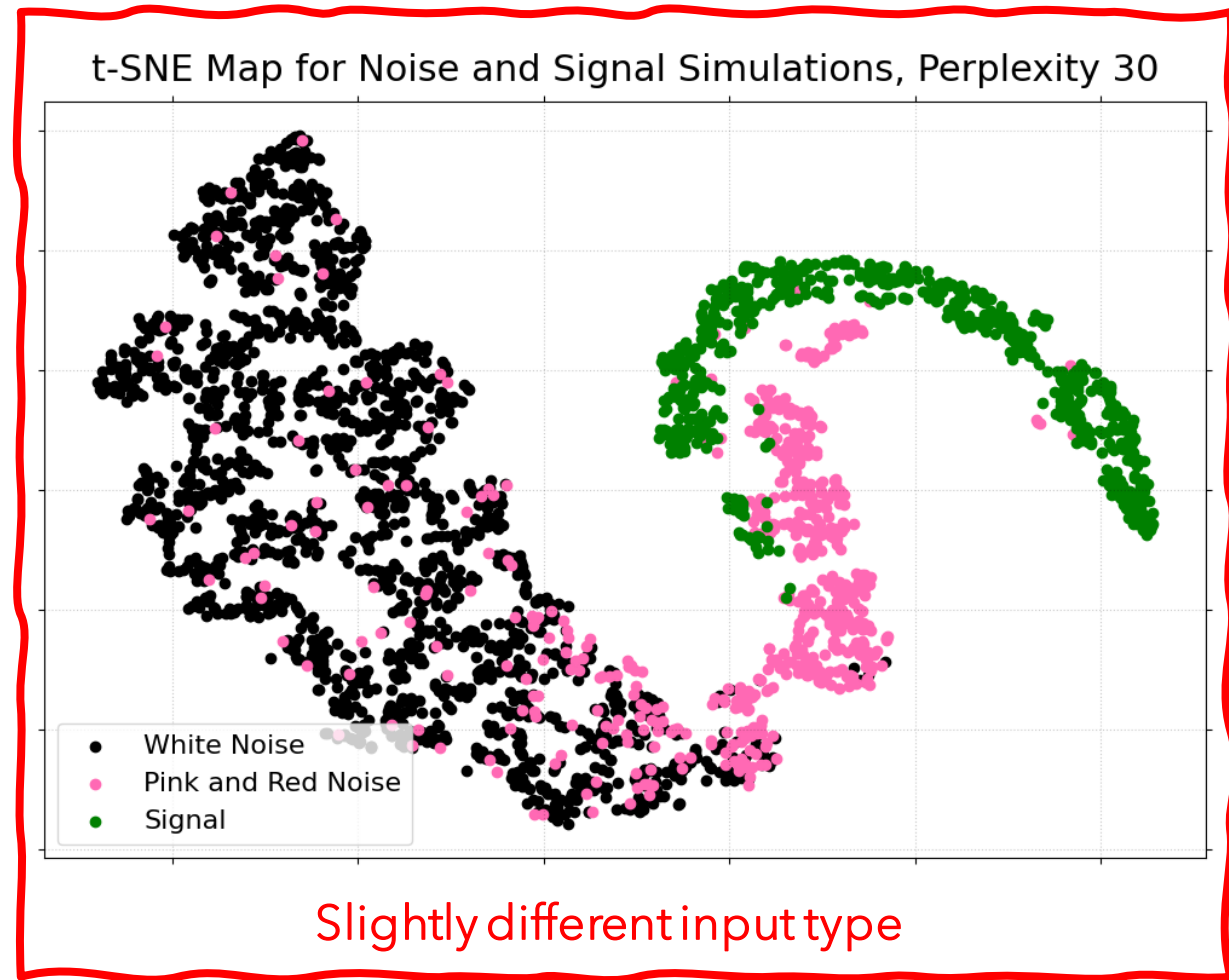
where  $P_i$  represents the conditional probability distribution over all other  $\{x_j\}$  given  $\{x_i\}$ , and  $H(P_i)$  is the Shannon entropy of  $P_i$  in bits [202].

# t-SNE, Simulations

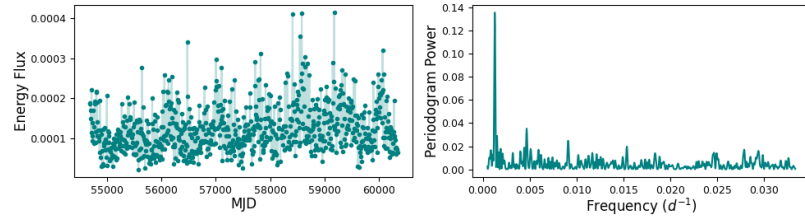
t-SNE Map for Noise and Signal Simulations, Perplexity 30



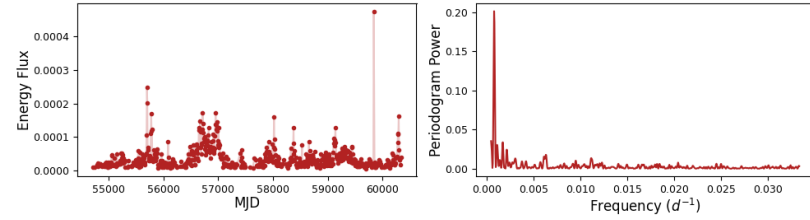
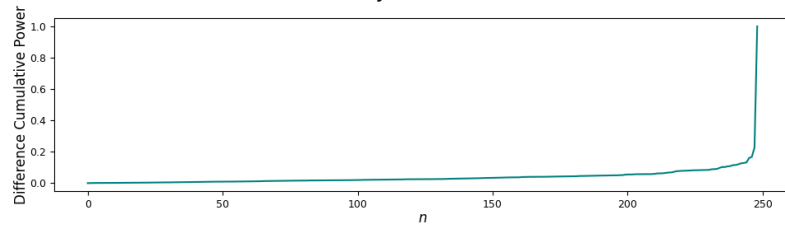
t-SNE Map for Noise and Signal Simulations, Perplexity 30



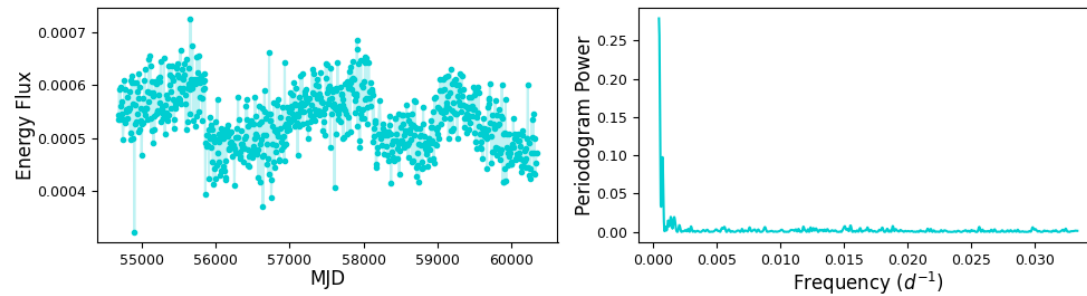
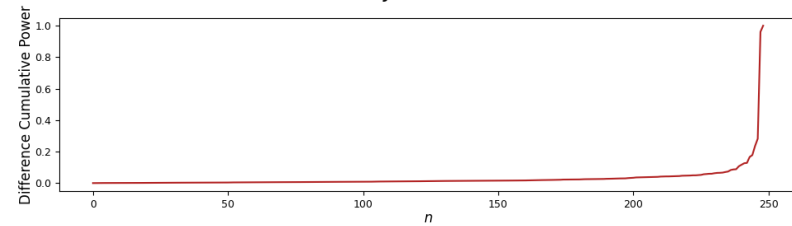
# t-SNE, Sources



4FGL J1555.7+1111



4FGL J1146.9+3958



4FGL J2021.5+4026

